

The heterogeneity of the RNA degradation exosome in *Sulfolobus*

Chamindri Witharana

Medical Laboratory Science Degree Program, Faculty of Medicine, University of Ruhuna, Galle, Sri Lanka

Corresponding author: Chamindri Witharana
<changa1623@yahoo.com>

Introduction

RNA is necessary for protein synthesis and for gene regulation in all living organisms. Most RNA molecules are transcribed as precursors which are then matured by ribonucleases (RNases) and RNA modification enzymes. Often large multiprotein complexes are responsible for the maturation and for the degradation of various RNA molecules in the cell. The general mechanisms of RNA processing and degradation are highly conserved and include endonucleolytic cleavages, posttranscriptional modification at the 3'-end (RNA tailing) and exoribonucleolytic degradation or trimming in 3'-5' direction or in 5'-3' direction (for recent reviews see Refs (1-3). Controlled RNA degradation as a part of the posttranscriptional gene regulation is especially important for unicellular, prokaryotic microorganisms, which are exposed to changing environmental conditions. Prokaryotes are a highly heterogeneous group which include bacteria and Archaea. Archaea show morphological similarities to bacteria, but are closely related phylogenetically to eukarya than to bacteria (4). They also show a strong similarity to eukarya at the molecular level, for example in the mechanisms of replication, transcription and translation. Archaeal mRNA, however, is more similar to bacterial mRNA: it is generally intron-less and lacks a long stabilising poly (A)-tail at the 3'-end as well as a methylguanosine cap at the 5'-end. In accordance with this, the mechanisms of RNA degradation in Archaea show strong similarities to those operating in bacteria (2). For example, the archaeal protein complex named exosome is structurally and functionally similar to the bacterial polynucleotide phosphorylase (PNPase) (5-8). The bacterial PNPase and the archaeal exosome show structural similarities to

the eukaryotic nine-subunit exosome (9), but there are important functional differences between the eukaryotic and prokaryotic exosome-like machineries. The activity of the eukaryotic nine subunit exosome is due to a tenth subunit with similarity to the bacterial RNase R, while its PNPase-like, nine-subunit core is catalytically inactive (10). The eukaryotic ten-subunit exosome that functions as a hydrolytic 3'-5' exoribonuclease and an endoribonuclease (11,12) is essential and participates in various RNA processing and RNA degrading pathways both in the nucleus and in the cytoplasm (13,14). Eukaryotic RNAs are intended for exoribonucleolytic 3'-5' degradation by the addition of short poly (A) tails. This destabilizing polyadenylation is performed by specialized protein complexes that are different from the eukaryotic exosome (15,16). In contrast, both the bacterial PNPase and the archaeal nine subunit exosome are phosphorolytic 3'-5' exoribonucleases, which also can use NDPs to synthesize destabilizing, heteropolymeric RNA tails, which are used as loading platforms for exo-ribonucleases (6,17,19). In Archaea lacking the exosome, RNA is not post-transcriptionally modified at the 3'-end (19). In these exosome-less Archaea, RNA is either exoribonucleolytically degraded in 3'-5' direction by a homologue of bacterial RNase R (in halophiles) or seems to be exclusively degraded in 5'-3' direction by a homologue of the bacterial RNase J (in some methanogenic Archaea) (20,21). Like in Bacteria, in Archaea degradation in 5'-3' direction is inhibited by a 5'-triphosphate and is performed by RNase J homologues (22,23). The endoribonucleolytic mechanisms, which are of central importance for RNA degradation in Bacteria (3,24) are still not explored in Archaea. The recently described, endonucleolytically

active RNase J homologues in methanogens are good candidates for principle endoribonucleases in the third domain of life (21). The existence of the archaeal exosome was proposed by bioinformatic analyses based on its similarity to the eukaryotic exosome (25) and was verified by co-immunoprecipitation from the thermoacidophilic archaeon *Sulfolobus solfataricus* (26). Later, its existence *in vivo* was verified for two further archaeal species, *Methanothermobacter thermoautotrophicus* and *Thermococcus kodakarensis* (27,28). Major components of the archaeal exosome are the orthologs of the eukaryotic exosomal subunits Rrp41, Rrp42, Rrp4 and Csl4 forming the nine-subunit form of the archaeal complex, and the archaeal DnaG protein, the function of which in respect to RNA is still unknown. The structure and the catalytic mechanism of the reconstituted archaeal nine-subunit exosome are well understood. It is built of a phosphorolytically active hexameric ring containing the subunits Rrp41 (harbouring the active centre) and Rrp42, to which a trimeric cap of the RNA-binding proteins Rrp4 and/or Csl4 is bound. It performs metal-dependent phosphorolysis of RNA in the presence of inorganic phosphate (Pi) and Mg₂Cl, and synthesizes RNA using NDPs without a template (5-8, 29-31).

In vitro, the amounts of Pi, NDPs and Mg₂Cl determine the direction of the reaction (32). However, little is known however about the regulation of the functions of the archaeal exosome *in vivo*. The function of the RNA-binding cap was investigated *in vitro* using recombinant exosomes of several archaea belonging to the genera *Sulfolobus*, *Pyrococcus* and *Archaeoglobus*. So far, homomeric caps composed of Rrp4 or Csl4 were studied in detail. Generally, the presence of Rrp4 or Csl4 increases RNA binding and the efficiency of RNA degradation and RNA synthesis by the archaea exosome (7,8,18, 32-34). Recently we have shown that Rrp4 and Csl4 confer different substrate specificities to the archaeal exosome and that Rrp4 strongly prefers poly(A). Although *S. solfataricus* does not have poly(A) tails, poly(A) stretches are present in the heteropolymeric RNA tails synthesized by the

exosome (19). Furthermore, the GC content of the *S. solfataricus* genome is 37% and short poly(A) stretches are present in its mRNAs. These poly(A) stretches are most probably the determinants recognized by the Rrp4-containing exosome, since the presence of a naturally occurring, adenine-rich RNA tail enhanced the degradation of a synthetic, heteropolymeric RNA by the exosome carrying a homomeric cap built of Rrp4 but not of Csl4. Although it was shown *in vitro* that the reconstituted exosome of *Archaeoglobus fulgidus* can carry a heteromeric cap containing Rrp4 and Csl4 (7), the cap composition of the archaeal exosome was not studied *in vivo* so far. Changes in the composition of the exosome may influence not only its substrate specificity, but also the interaction with other proteins and even its subcellular localization. The majority of the active site containing subunit Rrp41 is localized at the periphery of the *S. solfataricus* cell and is detectable in the insoluble fraction of a cell-free extract. DnaG was also detected at the cell periphery and is essentially insoluble. The aim of this work was to analyze the composition of the soluble and the insoluble exosomes. We found that the exosome contains heteromeric, Rrp4 and Csl4 containing caps *in vivo*, and that exosomes with different sedimentation behaviours differ in their composition.

Material and Methods

Cell growth and fractionation experiments

S. solfataricus P2 was grown in a 10 l fermenter at 75°C in a rich medium under air supply as described. Cells (470 mg wet pellet) were re-suspended in 1 ml lysis buffer containing 20 mM MES (2-(N-morpholino)ethanesulfonic acid), pH 6.5, 0.5 mM EDTA, 1 mM PMSF, 2 mM DTT, DNase I and 1 mM protease inhibitor cocktail (Sigma Aldrich, Germany), and sonified. After lysis, 500 mM ammonium chloride and 10 mM magnesium acetate were added and the cell free extract was clarified by centrifugation at 2500 g for 20 min at 4°C. To obtain S100 and P100 fractions, the supernatant was subjected to ultra centrifugation at 100,000 g for 1 h at 4°C. Prior to analysis, the pellet

fraction was re-suspended in 1 ml of lysis buffer containing 500 mM ammonium chloride and 10 mM MgCl₂. Membranes were removed at 13,000 g. Fractionation in 15-70% sucrose density gradient containing 500 mM ammonium chloride and 10 mM magnesium acetate was performed.

SDS-PAGE and Western blot analysis

Proteins were separated in 12% SDS-PAGE and silver stained, or blotted onto a nitrocellulose membrane and hybridized with rabbit sera directed against Rrp41 (26), DnaG (18), Rrp4 and Csl4 (Davids Biotechnologie GmbH, Regensburg, Germany). The secondary antibody was anti-rabbit IgG conjugated with peroxidase (Pierce), and the Lumi-Light Western blotting substrate (Roche Diagnostics GmbH) was used for detection. The bands were quantified using Peqlab Fusion SL 4 instrument and the corresponding software.

Co-immunoprecipitation and depletion experiments

Co-immunoprecipitation and depletion experiments with polyclonal antibodies covalently coupled to protein A-Sepharose were performed as previously described (18). We used 800 ml of cell-free extract or 600 ml density gradient fractions (pooled were 300 ml of fractions 6 and 7 or fractions 12 and 13) and 0.04 g of beads coupled with antibodies in 150 ml phosphate buffered saline were used.

Reconstitution of exosomal complexes

PCR was performed with genomic DNA of *S. solfataricus*, the amplicates were cloned in pDrive (Qiagen) and re-cloned between the XhoI and NdeI restriction sites of the pET-15b expression vector. Rrp4 deletion variants as well as the full-length subunits of the exosome Rrp41, Rrp42 (6) and Rrp4 (29) were over expressed in *Escherichia coli* BL21 (DE3) and purified by Ni-NTA affinity chromatography. To analyze the interaction of deletion variants of Rrp4 with the hexameric ring, the purified subunits were mixed together in nearly

equimolar amounts and were dialysed at room temperature in a buffer containing either 150 mM or 500 mM NaCl, 10 mM Tris pH 7, 5 mM MgCl₂, 0.5 mM EDTA, 5% Glycerol, 0.05% Tween 20, 0.2 mM DTT for 20 min. Then co-immunoprecipitation with Rrp41-specific antibodies followed by SDS-PAGE analysis was performed.

Results

Differences in the composition of the soluble and the insoluble exosomes

Previously we have shown by immunofluorescence that the majority of the *S. solfataricus* exosome is localized at the periphery of the cell. Consistent with this, only a minor part of Rrp41 was detected in the soluble, supernatant fraction (S100) and DnaG was detected only in the insoluble, pellet fraction (P100) after ultracentrifugation of the cell-free extract at 100,000 g. So far, the RNA-binding subunits of the exosome Rrp4 and Csl4 were not investigated in this respect. To address the question whether there are differences in the composition of the RNA binding caps of the soluble and the insoluble exosomes, antibodies were raised against recombinant Rrp4 and Csl4 of *S. solfataricus* and were used in quantitative Western blot analyses of the S100 and P100 fractions. DnaG and Rrp41 were also included in the analyses. In three independent experiments, 21 (+ or -) 3% of Rrp4 and 23 (+ or -) 3% of Rrp41 were detected in the S100 fraction. In contrast, Csl4 and DnaG were detected in the P100 fraction only (Figure 1A). Since the sensitivities of the antibodies used for detection of Csl4 and DnaG are lower than the sensitivities of the anti-Rrp41 and anti-Rrp4 antibodies (not shown), this result does not necessarily imply different subunit contents of the soluble and the insoluble exosomes, but confirms that the majority of the exosome is insoluble. To directly compare the compositions of the soluble and the insoluble exosomes, we decided to purify the exosome from the S100 and the P100 fractions by co-immunoprecipitation. The isolation of the exosome from the S100 fraction succeeded (see below), but we were not able to

immunoprecipitate the complex from the P100 fraction. Therefore we decided to use sucrose density gradient fractions and to compare the composition of exosomal complexes with different sedimentation behaviours. The majority of the exosome sediments with the membranes, but some exosome is also present in fractions of low density (soluble exosome) and in the middle of the gradient (part of the insoluble exosome co-sedimenting with ribosomal subunits). Since immunoprecipitation of the exosome from the membrane containing fraction 19 failed, we decided to compare the soluble exosome from fraction 6 to the insoluble exosome from fraction 12. We first removed the heavy membrane fraction with the Sla proteins and the associated exosome by centrifugation of the crude extract at 13,000 g. The supernatant containing the soluble components of the extract and particles with high molecular weight like the ribosomal subunits was then fractionated through a sucrose density gradient, and the fractions were analyzed for the presence of exosomal subunits by Western blot hybridization (Figure 1C). In agreement with the data in figure 1A, Rrp41 and Rrp4 were detected in fractions corresponding to soluble and insoluble components of the extract, while DnaG and Csl4 were detected only in the fractions with insoluble components. Using Rrp41-specific antibodies, we were able to isolate the soluble exosome from fraction 6 and the insoluble exosome from fraction 12 (Figure 2). SDS-PAGE analysis revealed the presence of following proteins in the elution fraction containing the soluble exosome: Rrp4, Rrp41, Rrp42, DnaG, and a protein larger than DnaG, which was identified as EF1-alpha by mass spectrometry (Figure 2A). The identity of DnaG was also confirmed by mass spectrometry. Figure 2B shows that the insoluble exosome from fraction 12 contains no EF1-alpha. A control experiment with a pre-immune serum was also performed using fraction 6 of the density gradient. No EF1-alpha and no DnaG were detected, neither by SDS-PAGE and silver staining, nor by mass spectrometry analysis (not shown).

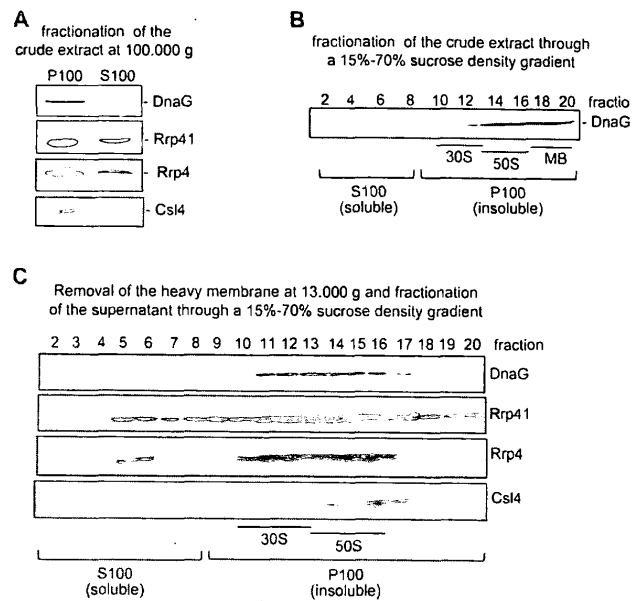


Figure 1: Detection of DnaG, Rrp41, Rrp4 and Csl4 in fractions of the *S. solfataricus* cell-free extract by Western blot analysis A) Western blot analysis of S100 and P100 fractions. Equal volume of the S100 and the P100 fractions were separated in 12% SDS-PAGE, blotted and hybridized with sera directed against the exosomal subunits indicated on the right side of the panels. B) Schematic representation of the sedimentation of the small (30S) and large (50S) ribosomal subunits, and of membranes (MB) with surface layer proteins in fractions of a sucrose density gradient with 500 mM salt. Shown is also the relationship between sucrose density gradient fractions and S100 and P100 fractions. The sedimentation of the exosome is shown on the example of DnaG detected by Western blotting of selected fractions. Fractionated was the crude extract C). The cell-free extract was subjected to low speed centrifugation to remove the membranes with the surface layer proteins and the associated exosome. The supernatant was fractionated through the sucrose density gradient and the fractions were analyzed for the presence of DnaG, Rrp41, Rrp4 and Csl4 by Western blot hybridization. The analyzed fractions are given above the panels the detected proteins are marked on the right side. The relationship between density gradient fractions, S100 and P100, and the sedimentation of the ribosomal subunits is given below the panels.

Since the exosomes from fractions 6 and 12 represent a minority of the exosome in *S. solfataricus* cells, questions arise about their functional relevance. To address this, we performed activity assays with the co-immunoprecipitated complexes. The assays were performed directly with the proteins bound to the protein A-Sepharose beads (18). Lanes 7 and 8 in figure 2C show that the soluble and the insoluble exosomes can degrade RNA. Thus, although present in low amounts, the soluble exosome is active. We verified that the exosome is a major RNA degrading enzyme in the soluble fraction of *S. solfataricus*: The RNA degrading activity of fraction 6 disappeared after depletion of the exosome by three rounds of co-immunoprecipitation with Rrp41-directed antibodies (Figure 2C, lanes 1 and 2). Similar results were obtained for the polyadenylation activity of fraction 6 and for fraction 12 (not shown). A comparison between figure 2A and B shows that in relation to the hexameric core composed of Rrp41 and Rrp42, more DnaG is present in the insoluble exosome from fraction 12 than in the soluble exosome from fraction 6. Csl4 was not clearly detected in the silver stained gels, but it was possible to detect it by Western blot hybridization. To analyze the differences in the composition of the RNA-binding caps of the soluble and the insoluble exosomes, the elution fractions shown in figure 2A and B were hybridized simultaneously with Rrp4- and Csl4-directed antibodies. Figure 2D shows that in relation to Rrp4, the insoluble exosome contains higher amounts of Csl4 than the soluble exosome. DnaG and Csl4 were not

detected by Western blot analysis in the S100 fraction (Figure 1A) and in fractions of low sucrose density like fraction 6 (Figure 1C), but were co-immunoprecipitated from those fractions (Figure 2A and D). This shows that the amounts of DnaG and Csl4 in S100 and in fraction 6 were under the limit of detection in the Western blot analysis, but it was possible to enrich these proteins during the immunoprecipitation procedure. In summary, Figure 2 shows that the soluble and the insoluble exosomes differ in their DnaG content and in the composition of the RNA-binding caps. The data also suggests an interaction between the soluble exosome and EF1-alpha. Both the soluble and the insoluble exosomes can degrade RNA, but their functional relevance is still unexplored.

To confirm an interaction between the soluble exosome and EF1-alpha by an independent experiment, we purified the exosome from the S100 fraction using DnaG-specific antibodies. The immunoprecipitated exosome contained Csl4, Rrp4, Rrp41, Rrp42, DnaG and EF1-alpha (Figure 3A). The identities of DnaG and EF1-alpha were confirmed by mass spectrometry. We assumed that only a part of the exosomal complexes present in the soluble fraction contain DnaG. Therefore, we decided to remove the DnaG containing exosome from the S100 fraction by three rounds of immunoprecipitation with the DnaG-specific antibodies, and then to purify the DnaG-less exosome from the depleted S100 fraction using Rrp41-specific antibodies. Figure 3B shows the Western blot analysis of the flow through (depleted S100 fraction) after each.

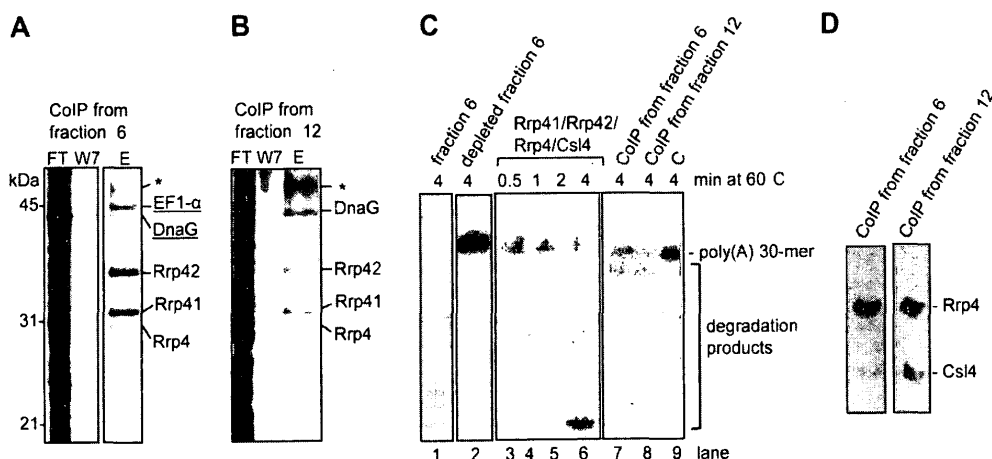


Figure 2: Exosomal complexes with different sedimentation behaviours are active and differ in their composition. A) and B) Silver stained SDS-gels showing proteins purified by coimmunoprecipitation (CoIP) with Rrp41-specific antibodies from different sucrose density gradient fractions. A) The soluble exosome was purified from fraction 6. B) The insoluble exosome was purified from fraction 12. FT, flow-through; W7, last, seventh washing fraction; E, elution fraction. The migration of marker proteins is marked (in kDa). Underlined proteins were identified by mass spectrometry, bands with known migration behaviour are marked with the names of the respective proteins. The band corresponding to antibodies is marked with an asterisk. C) Phosphor images of degradation assays with fraction 6 (lane 1), depleted fraction 6 (the flow-through after three rounds of immunoprecipitation of the exosome with Rrp41-specific antibodies (18); lane 2), exosomes reconstituted by mixing of equimolar amounts of Rrp41, Rrp42 and the RNA-binding proteins Rrp4 and Csl4 (lanes 3e6), the co-immunoprecipitated exosome from fraction 6 (lane 7), the co-immunoprecipitated exosome from fraction 12 (lane 8), and water (negative control C, lane 9), as indicated above the panels. The incubation time in minutes (min) is also indicated. The 50-labelled 30-meric poly(A) RNA and the degradation products are marked on the right side. D) Western blot analysis of the elution fractions are shown in A) and B). To estimate the relative amounts of Csl4 and Rrp4, the membranes were hybridized simultaneously with Csl4- and Rrp4-directed antibodies. The detected proteins are marked on the right side.

Immunoprecipitation step. The removal of the exosome with DnaG specific antibodies led to a strong decrease in the intensity of the Rrp41 signal. The remaining exosome was purified with Rrp41- specific antibodies. The SDS-PAGE analysis of the elution fraction (Figure 3C) revealed bands with similar migration when compared to Figure 3A. The presence of Csl4 and DnaG in the elution fraction shown in Figure 3C was confirmed by mass spectrometry. The band of low intensity above DnaG was identified as TIP49 protein, showing that EF1-alpha was

already removed together with the exosome during the depletion with the DnaG-specific antibodies. This result points to the possibility that the soluble exosome interacts with different proteins. TIP49 was not detected as a minor protein in the EF1-alpha containing gel slices analyzed by mass spectrometry. This protein was also not found in the corresponding gel slices in a control experiment with the pre-immune serum (not shown).

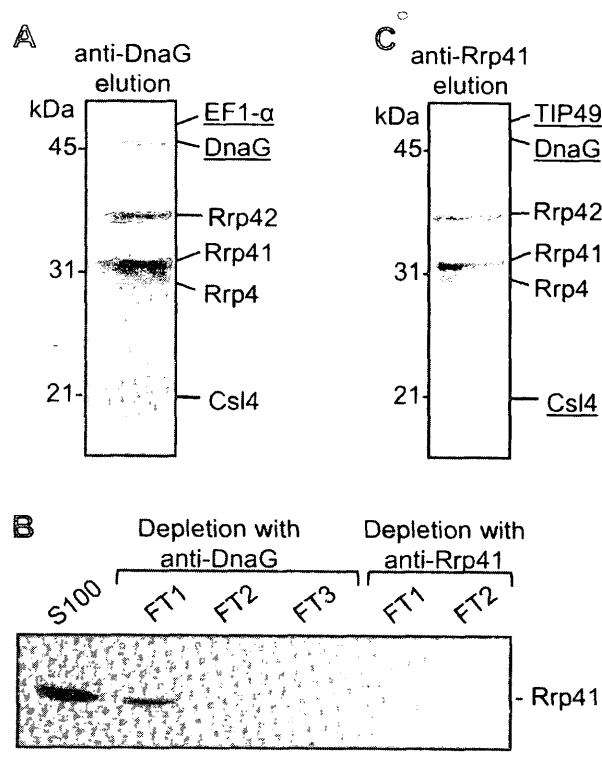


Figure 3: Co-immunoprecipitation (CoIP) of EF1-alpha with the soluble exosome using DnaG-specific antibodies. The S100 fraction was subjected to three rounds of CoIP with DnaG-specific antibodies (anti-DnaG). Subsequently, two rounds of CoIP with Rrp41- specific antibodies (anti-Rrp41) were performed. A) Silver stained SDS-gels showing the proteins, which were co-precipitated during the first CoIP round with anti-DnaG (anti-DnaG elution). B) Western blot analysis of the flow-through fractions (FT) after each CoIP round. The antibodies used for depletion by CoIP are marked above the panels. The FT fractions (depleted S100) were separated on a 12% SDS-PAGE and hybridized with anti-Rrp41. The detected Rrp41 is marked on the right side of the panel. C) Silver stained SDS-gels showing the

proteins, which were co-precipitated during the first CoIP round with anti-Rrp41 (anti-Rrp41 elution). For further description see Figure 2B.

Figure 3 shows that, it was not possible to completely remove the DnaG-containing exosome from the S100 fraction after three rounds of co-immunoprecipitation with DnaG specific antibodies. On the other hand, it strongly suggests that the most of the exosomes in the soluble fraction are associated with DnaG, since it was not possible to enrich exosomes without DnaG. Based on Figure 2 and 3, we conclude that DnaG and Csl4 are integral parts of the soluble exosome. Furthermore, the data supports the interaction between EF1-alpha and the exosome and suggests that DnaG and EF1-alpha are present together in the soluble exosome.

Rrp4 and Csl4 form heteromeric RNA-binding caps *in vivo*

Figure 2C suggests that exosomes with different sedimentation behaviours have differences in the composition of the RNA-binding cap. However, it was still not clear whether Rrp4 and Csl4 are present together in the exosome. The RNA-binding cap of the exosome of *A. fulgidus* can be composed of Rrp4, Csl4 or both Rrp4 and Csl4 *in vitro* (7). However, the existence of archaeal exosomes with heteromeric RNA-binding caps containing Rrp4 and Csl4, was not shown *in vivo* so far. To study the *in vivo* composition of the RNA-binding cap, the exosome was immunoprecipitated with Rrp4-specific antibodies or with Csl4-specific antibodies from *S. solfataricus* cell-free extracts and from S100 fraction. The elution fractions were tested for the presence of Csl4 and Rrp4, respectively. To ensure detection of Csl4, 1.2 g

of cells (wet pellet) were lysed in 1 ml of buffer, and the clarified cell-free extract (supernatant after centrifugation at 2500 g) or the corresponding S100 fraction was used for co-immunoprecipitation. The immunoprecipitated proteins were eluted in 40 ml, and the complete elution fraction was loaded. Figure 4A and B shows that Csl4 is coimmunoprecipitated together with the exosome when Rrp4-specific antibodies are used, and vice versa. The identities of Csl4 and Rrp4 were confirmed by mass spectrometry. Thus, the archaeal exosome contains heteromeric RNA-binding caps *in vivo*, and such caps are present in the soluble exosome. Since Rrp4 and Csl4 confer different substrate specificities to the exosome and may also be responsible for the interaction with different protein partners, it is interesting to know whether different RNA-binding caps exist *in vivo* consisting of Rrp4 only, Csl4 only, and Rrp4 and Csl4 in different relative amounts. We assumed that if heterogeneous RNA-binding caps are present, they should be differently enriched in immunoprecipitation experiments with Rrp4- or Csl4-directed antibodies. The elution fractions shown in Figure 4A and B suggest that similar relative amounts of Rrp4, Rrp41 and Rrp42 were isolated with the two different antibodies, but higher amounts of Csl4 were isolated with the Csl4-directed antibodies than with the Rrp4-directed antibodies. Figure 4C confirms that different relative amounts of Rrp4 and Csl4 are immunoprecipitated from the S100 fraction when the two different antibodies are used. These results confirm that Rrp4 and Csl4 are parts of protein complexes *in vivo* and do not exist as monomers. From the results in Figure 4 we conclude that exosomes with heterogeneous RNA-binding caps are present in the soluble fraction of *S. solfataricus*.

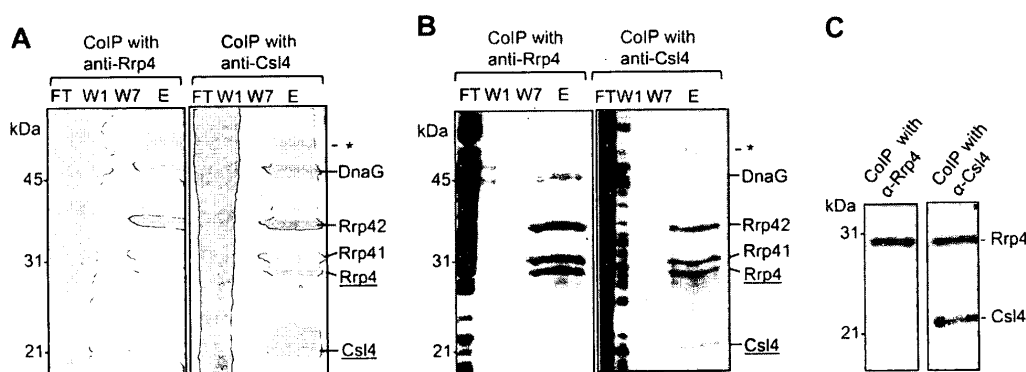


Figure 4: *In vivo* analysis of the RNA-binding cap of the *S. solfataricus* exosome. A) and B) show silver stained gels, C shows Western blot analysis. A) Co-immunoprecipitation (CoIP) experiments with anti-Rrp4 and anti-Csl4 antibodies from a clarified cell-free extract. B) CoIP with anti-Rrp4 and anti-Csl4 antibodies from S100 fractions. W1, first elution fraction. For further descriptions see Figure 2C. Western blot analysis of exosomes immunoprecipitated from S100 fractions with anti-Rrp4 and anti-Csl4 antibodies (marked above the panels). To estimate the relative amounts of Csl4 and Rrp4 in the immunoprecipitated complexes, the membranes were hybridized simultaneously with Csl4- and Rrp4-directed antibodies. The detected proteins are marked on the right side.

Discussion

Our approach to purify the archaeal exosome using antibodies directed against different subunits and using different protein fractions was helpful to uncover the heterogeneity in the composition of this protein complex in *S. solfataricus*. We found that the content of the soluble exosome differs from the content of the insoluble exosome which sediments in the middle of sucrose density gradients together with ribosomal subunits. Since the majority of the exosome co-sediments with membranes, the complexes analyzed in this work represent a minor part of the exosome of *S. solfataricus*. Nevertheless this minor part should be of functional importance, since both the soluble and the insoluble exosomes were active. The functions of archaeal exosomes with different sedimentation properties are still not explored, but it can be speculated that the soluble exosome is important for the metabolism of mRNAs and tRNAs present in the soluble fraction, while the exosome which co-sediments with ribosomal subunits may be involved in rRNA processing. In this respect, the differences in the protein composition of the soluble and the insoluble exosomes may reflect the need to interact with different RNA substrates and different accessory proteins. So far the archaeal nine-subunit exosome was intensely studied *in vitro*, but little is known about its interactions with other proteins. Association of the archaeal DnaG

protein with the exosome was reported for several archaeal species (18,27,28), but the function of DnaG in this context remains unclear. Recently it was shown that DnaG exhibits primase activity and it was proposed that archaea harbour both an eukarya-like and a bacteria-like primase. This might explain the high conservation of DnaG in archaea, even in species lacking the exosome. Nevertheless, DnaG seems to be of fundamental importance for the archaeal exosome. Our results show that although it is present in lower amount in soluble exosomes of *S. solfataricus* than in exosomes of higher sedimentation coefficient, the majority or all soluble exosomes contain DnaG. Accordingly to our data, DnaG is the major interaction partner of the exosome with higher sedimentation coefficient, while the soluble exosome interacts with additional proteins. The copurification of EF1-alpha with the soluble exosome in three biologically independent experiments, using two different sera (Rrp41-specific and DnaG-specific) and different protein fractions (S100 or sucrose density gradient fraction), strongly suggests a functional interaction between EF1-alpha and the protein complex. The co-purification of TIP49 with the residual soluble exosome after depletion with DnaG-specific antibodies indicates that the soluble exosome may interact with different minor protein partners. The specificity of the copurification of the exosome and TIP49 remains to be verified. Interaction of the exosome with other proteins was reported for several archaeal species. The DnaG-containing exosome was detected in a high molecular mass complex with the tRNA-intron endonuclease in *M. thermoautotrophicus* (27). On the other hand, it was co-purified with an rRNA biogenesis factor (FAU-1 protein) and a protein with unknown function (TK0790) in *T. kodakarensis* (28). In another study, the activity of the *Pyrococcus abyssi* exosome was shown to be affected *in vitro* by two RNA binding proteins, PaSBDS and PaNip7, and it was shown that PaNip7 associates with the exosome in the absence of RNA. Our data strongly support the interaction between the exosome and EF1-alpha in *S. solfataricus*. The archaeal EF1-alpha is involved in translational elongation and

termination, and mRNA surveillance pathways, suggesting that it may link the release of mRNA from the ribosome to its tailing and/or degradation by the exosome. The simultaneous presence of Rrp4 and Csl4 in the RNA-binding cap of the archaeal exosome *in vivo* probably ensures its interaction with different transcripts and protein partners. Different Rrp4/Csl4 stoichiometries in different fractions of the exosome probably influence the functions of the complex. It was shown for *Archaeoglobus*, *Pyrococcus* and *Sulfolobus*, that Rrp4 and Csl4 differently influence the interaction of the exosome with RNA. Little is known, however, about the *in vivo* stoichiometry of these subunits in the heterogeneous exosomal complexes and about the specific function of these proteins and their individual domains. The comparison of exosomes isolated with anti-Rrp4 and anti-Csl4 antibodies suggests that in both cases, when compared to the amounts of Rrp41 and Rrp42 forming the catalytic hexamer, quite similar amounts of Rrp4, but very different amounts of Csl4 were isolated (Figure 4). Since the presence of monomeric Csl4 was excluded, the high amount of Csl4 isolated with the anti-Csl4 antibodies is probably a part of the co-precipitated exosome. In such a case, however, our results are not compatible with a trimeric structure of the RNA-binding cap which is composed of Rrp4 only, Csl4 only or Rrp4 and Csl4 in different stoichiometries. Such a trimeric structure implies that enrichment of Csl4 by co-immunoprecipitation should result in less Rrp4 in the elution fraction and vice versa. The results shown in Figure 4 rather imply that a small amount of the exosome with the usual Rrp41/Rrp42/Rrp4 stoichiometry but containing an excess of Csl4 is enriched by co-immunoprecipitation with Csl4-specific antibodies. The exosome which is immunoprecipitated with Rrp4-specific antibodies seems to contain Rrp41, Rrp42 and Rrp4 in similar amounts and Csl4 in very low amounts, resembling the reconstituted *S. solfataricus* exosome. The possibility that some Csl4 aggregates, which do not interact with the exosome, were co-precipitated with the Csl4-specific antibodies should be excluded, since Csl4-poor exosomes and Csl4-rich exosomes

were also purified with Rrp41-antibodies (see Figure 2). Thus, Csl4-rich exosomes and Csl4-poor exosomes exist *in vivo* and can be separated in sucrose density gradients. Based on this, it is tempting to speculate that individual domains in the RNA-binding cap of the exosome are involved in the regulation of the dual function of the exosome as an exoribonuclease and an RNA tailing enzyme in archaea.

Conclusions

In this study we showed the existence of RNA exosomes with heterogeneous composition in the archaeon, *S. solfataricus*. The different relative amounts of DnaG and Csl4 found in the soluble and the insoluble exosomes suggest that these proteins determine the sedimentation properties of the complex. We also found that although present in lower amounts, DnaG is an integral part of the soluble exosome, and that the soluble exosome interacts with EF1- α . The presence of heteromeric, Rrp4 and Csl4 containing, RNA binding caps *in vivo*, the different relative amounts of Rrp4 and Csl4 in soluble and insoluble exosomes, and the different effects of DKHRrp4 on the activities of the hexameric ring *in vitro* strongly suggest that the RNA-binding cap is involved in the regulation of the functions of this RNA-degrading and RNA-tailing protein complex.

Acknowledgements

This work was supported by DFG, grant K1563/27-1 and IRTG "Enzymes and multi-enzyme complexes acting on nucleic acids".

References

1. C Condon. Maturation and degradation of RNA in bacteria, *Curr. Opin. Microbiol.* (2007);**10**:271-278.
2. E Evguenieva-Hackenberg, G. Klug, RNA degradation in Archaea and Gramnegative bacteria different from *Escherichia coli*, *Prog. Mol. Biol. Transl. Sci.* 2009;**85**:275-317.
3. JG Belasco. All things must pass: contrasts and commonalities in eukaryotic and bacterial mRNA decay. *Nat. Rev. Mol. Cell. Biol.* 2010;**11**:467-478.

4. CR Woese, GE Fox, Phylogenetic structure of the prokaryotic domain: the primary kingdoms. *Proc. Natl. Acad. Sci. U.S.A.* 1977;**74**:5088-5090.
5. E Evguenieva-Hackenberg, The archaeal exosome, *Adv. Exp. Med. Biol.* 702 (2010) 29e38.
6. E Lorentzen, P Walter, S Fribourg, E Evguenieva-Hackenberg, G Klug, E Conti. The archaeal exosome core is a hexameric ring structure with three catalytic subunits, *Nat. Struct. Mol. Biol.* 2005;**12**:575-581.
7. K Büttner, K Wenig, KP Hopfner. Structural framework for the mechanism of archaeal exosomes in RNA processing, *Mol. Cell* 2005;**20**:461-471.
8. CR Ramos, CL Oliveira, IL Torriani, CC Oliveira. The Pyrococcus exosome complex: structural and functional characterization. *J. Biol. Chem.* 2006;**281**:6751e6759.
9. Q Liu, JC Greimann, CD Lima. Reconstitution, activities, and structure of the eukaryotic RNA exosome, *Cell* 127 (2006) 1223e1237 Erratum in: *Cell* 2007;**131**:188-189.
10. ADziembowski, E Lorentzen, E Conti, B Séraphin. A single subunit, Dis3 is essentially responsible for yeast exosome core activity. *Nat. Struct. Mol. Biol.* 2007;**14**:15-22.
11. A Lebreton, R Tomecki, A Dziembowski, B Séraphin. Endonucleolytic RNA cleavage by a eukaryotic exosome, *Nature* 2008;**456**:993-996.
12. D Schaeffer, B Tsanova, A Barbas, FP Reis; EG Dastidar, M Sanchez-Rotunno, CM Arraiano, A van Hoof. The exosome contains domains with specific endoribonuclease, exoribonuclease and cytoplasmic mRNA decay activities. *Nat. Struct. Mol. Biol.* 2009;**16**:56-62.
13. P Mitchell, E Petfalski, A Shevchenko, M Mann, D Tollervey. The exosome: a conserved eukaryotic RNA processing complex containing multiple 30/50 exoribonucleases, *Cell* 1997;**91**:457-466.
14. C Allmang, J Kufel, G Chanfreau, P Mitchell, E Petfalski, D Tollervey. Functions of the exosome in rRNA, snoRNA and snRNA synthesis. *EMBO J* 1999;**18**:5399-5410.
15. J LaCava, J Houseley, C Saveanu, E Petfalski, E Thompson, A Jacquier, D Tollervey, RNA degradation by the exosome is promoted by a nuclear polyadenylation complex, *Cell* 2005;**12**:713-724.
16. S Vanáčová, J Wolf, G Martin, D Blank, S Dettwiler, A Friedlein, H Langen, G Keith, W Keller. A new yeast poly(A) polymerase complex involved in RNA quality control. *PLoS Biol.* 2005;**6**:189.
17. BK Mohanty, SR Kushner. Polynucleotide phosphorylase functions both as a 3'-5' exonuclease and a poly(A) polymerase in Escherichia coli. *Proc. Natl. Acad. Sci. U.S.A.* 2000;**97**:11966-11967.
18. P Walter, F Klein, E Lorentzen, A Ilchmann, G Klug, E Evguenieva-Hackenberg, Characterization of native and reconstituted exosome complexes from the hyperthermophilic archaeon *Sulfolobus solfataricus*, *Mol. Microbiol.* 2006;**62**:1076-1089.
19. V Portnoy, E Evguenieva-Hackenberg, F Klein, P Walter, E Lorentzen, G Klug, G Schuster. RNA polyadenylation in Archaea: not observed in Haloferax while the exosome polynucleotidylates RNA in *Sulfolobus*, *EMBO Rep.* 2005;**6**:188-1193.
20. V Portnoy, G Schuster, RNA polyadenylation and degradation in different Archaea: roles of the exosome and RNase R. *Nucleic Acids Res.* 2006;**34**:5923-5931.
21. S Levy, V Portnoy, J Admon, G Schuster. Distinct activities of several RNase J proteins in methanogenic archaea. *RNA Biol.* 2011;**8**:1073-1083.
22. N Mathy, L Bénard, O Pellegrini, R Daou, T Wen, C Condon, 5'-to-3' exoribonuclease activity in bacteria: role of RNase J1 in rRNA maturation and 5' stability of mRNA. *Cell* 2007;**129**:681-692.
23. D Hasenöhrl, R Konrat, U Bläsi, Identification of an RNase J ortholog in *Sulfolobus solfataricus*: implications for 50-to-30 directional decay and 5'-end protection of mRNA in Crenarchaeota. *RNA* 2011;**17**:99-107.
24. K Shahbadian, A Jamalli, L Zig, H Putzer, RNase Y, A Novel. Endoribonuclease, initiates riboswitch turnover in *Bacillus subtilis*. *EMBO J.* 2009;**28**:3523-3533.
25. EV Koonin, YI Wolf, L Aravind. Prediction of the archaeal exosome and its connections with the proteasome and the translation and transcription machineries by a comparative-genomic approach. *Genome Res.* 2001;**11**:240-252.

26. E Evguenieva-Hackenberg, P Walter, E Hochleitner, F Lottspeich, G Klug. An exosome-like complex in *Sulfolobus solfataricus*. *EMBO Rep.* 2003;4:889-893.
27. MH Farhoud, HJ Wessels, PJ Steenbakkens, S Mattijssen, RA Wevers, BG van Engelen, MS Jetten, JA Smeitink, LP van den Heuvel, JT Keltjens. Protein complexes in the archaeon *Methanothermobacter thermoautotrophicus* analyzed by blue native/ SDS-PAGE and mass spectrometry. *Mol. Cell. Proteomics* 2005;4:1653-1663.
28. Z Li, TJ Santangelo, L Cubo nová, JN Reeve, Z Kelman. Affinity purification of an archaeal DNA replication protein network. *MBio* 2010;1:00221-002210.
29. E Lorentzen, A Dziembowski, D Lindner, B Seraphin, E Conti. RNA channelling by the archaeal exosome. *EMBO Rep.* 2007;8:470-476.
30. MV Navarro, CC Oliveira, NI Zanchin, BG Guimarães. Insights into the mechanism of progressive RNA degradation by the archaeal exosome. *J. Biol. Chem.* 2008;283:14120-14131.
31. C Lu, F Ding, A Ke. Crystal structure of the *S. solfataricus* archaeal exosome reveals conformational flexibility in the RNA-binding ring. *PLoS One* 2010;5.
32. E Evguenieva-Hackenberg, V Roppelt, P Finsterseifer, G Klug, Rrp4 and Csl4 are needed for efficient degradation but not for polyadenylation of synthetic and natural RNA by the archaeal exosome. *Biochemistry* 2008;47:13158-13168.